This is an open access article published under an ACS AuthorChoice License, which permits copying and redistribution of the article or any adaptations for non-commercial purposes.

NANO LETTERS

Letter

pubs.acs.org/NanoLett

Changes in the Morphology and Proliferation of Astrocytes Induced by Two Modalities of Chemically Functionalized Single-Walled Carbon Nanotubes are Differentially Mediated by Glial Fibrillary Acidic Protein

Manoj K. Gottipati,[†] Elena Bekyarova,[‡,§] Michael Brenner,[†] Robert C. Haddon,*[,‡,∥] and Vladimir Parpura*[,†,⊥]

[†]Department of Neurobiology, University of Alabama, Birmingham, Alabama 35294, United States

[‡]Departments of Chemistry and Chemical Engineering and Center for Nanoscale Science and Engineering, University of California, Riverside, California 92521, United States

[§]Carbon Solutions, Inc., Riverside, California 92507, United States

[∥]Department of Physics, King Abdulaziz University, Jeddah 21589, Saudi Arabia

[⊥]Department of Biotechnology, University of Rijeka, 51000 Rijeka, Croatia

Supporting Information

ABSTRACT: Alterations in glial fibrillary acidic protein (GFAP) levels accompany the changes in the morphology and proliferation of astrocytes induced by colloidal solutes and films of carbon nanotubes (CNTs). To determine if GFAP is required for the effects of CNTs on astrocytes, we used astrocytes isolated from GFAP null mice. We find that selected astrocytic changes induced by CNTs are mediated by GFAP, i.e., perimeter, shape, and cell death for solutes, and proliferation for films.

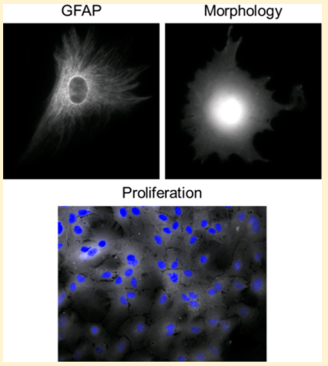

KEYWORDS: *Carbon nanotubes, graft copolymers, astrocytes, glial fibrillary acidic protein, knockout, morphology, proliferation, death*

Carbon nanotubes (CNTs) have emerged as a promising material in biomedicine, especially in neural prosthetics.[1,2] CNTs can be applied to neural cells as colloidal solutes or used as strata upon which cells can attach and grow. Single-walled CNTs chemically functionalized with polyethylene glycol (SWCNT-PEG), which renders them water-soluble, have been shown to modulate the morpho-functional properties of both neurons[3] and astrocytes[4] in culture. The application of SWCNT-PEG as colloidal solutes also affected neuronal morphology *in vivo* and improved locomotor recovery in an acute spinal cord injury rat model.[5] In addition to application as colloidal solutes, SWCNT-PEG can be sprayed onto hot glass coverslips to form retainable films, which also modulate the morpho-functional properties of neurons[6] and astrocytes.[7] These films also cause an increase in the rate of proliferation of astrocytes.[7] CNT films have shown much promise as a coating material for standard tungsten or stainless steel wire electrodes in brain-machine interface (BMI) applications; their use resulted in enhanced neuronal stimulation and recordings, both *in vitro* and *in vivo*.[8,9] The above changes in the properties of astrocytes induced by the two modalities of SWCNT-PEG, solutes and films, were associated with changes in the immunoreactivity (ir) of glial fibrillary acidic protein (GFAP). Since GFAP may contribute to both astrocytic process formation and inhibit proliferation,[10] the question arose whether GFAP is necessary for the morphological and proliferative changes of astrocytes induced by the different CNT modalities, or if the changed expression of GFAP is an independent event. To address this issue, we used a GFAP knockout (KO) mouse model[11] and assessed the morphological and proliferative characteristics of astrocytes. We observed that the changes in the size, shape, proliferation, and cell death of astrocytes caused by the two modalities of SWCNT-PEG are differentially mediated by GFAP. This indicates that the cellular effects exerted by CNTs are likely mediated by distinct intracellular molecular transduction pathways, a subset of which involves GFAP.

Received: December 28, 2013
Revised: May 23, 2014
Published: May 29, 2014

 © 2014 American Chemical Society dx.doi.org/10.1021/nl4048114 | *Nano Lett.* 2014, 14, 3720−3727

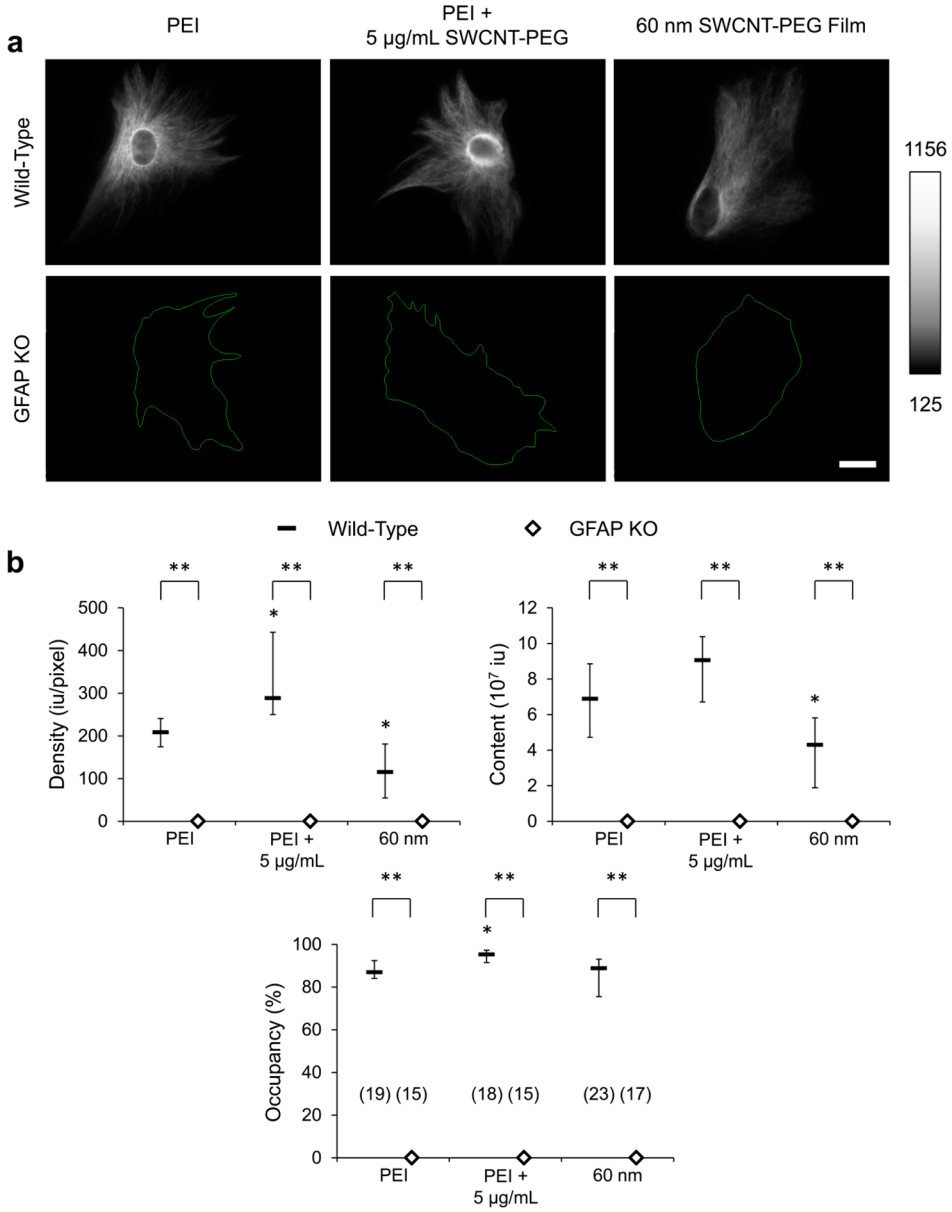

Figure 1. Both solute and film modalities of SWCNT-PEG induce functional changes in wild-type astrocytes, as seen by the changes in cellular GFAP immunoreactivity (GFAP-ir) parameters. (a) Images of wild-type and GFAP KO astrocytes in culture plated onto the PEI-coated coverslips in the absence and presence of the SWCNT-PEG solute (5 μg/mL) and onto the 60 nm thick SWCNT-PEG films, labeled for GFAP using indirect immunocytochemistry. The green traces in the GFAP KO panel represent the outline of the astrocytes based on the corresponding β-Ala-Lys-N$_\varepsilon$-AMCA images (not shown; but see Supporting Information, Figure S1) disclosing cytoplasm, i.e., total cell area. Scale bar, 20 μm. Gray scale is a linear representation of the fluorescence intensities of the pixels in the images, expressed in fluorescence intensity units (iu). (b) Summary graphs showing the median effects of the CNT modalities on GFAP-ir parameters. Density is shown in fluorescence intensity units (iu) per area (pixel). The number of astrocytes studied in each condition is given in parentheses in the occupancy graph. The boxes and diamonds represent medians with interquartile range (IQR) of wild-type and GFAP KO astrocytes, respectively. The Kruskal–Wallis one-way ANOVA (KWA) followed by the Dunn's test was used for the comparison between the different conditions (CNT modalities) in each group (wild-type or GFAP KO astrocytes); *p < 0.05, a statistical difference when compared to the cells plated onto the PEI-coated coverslips within the same group. The Mann–Whitney U-test was used for the comparison between wild-type and GFAP KO astrocytes in each condition; the differences are marked by the brackets; **p < 0.01.

The SWCNT-PEG graft copolymers were prepared using a procedure described elsewhere,[4,12] and an aqueous solute/dispersion was obtained by ultrasonication. Uniform retainable films of these graft copolymers were made by spraying them onto hot precleaned glass coverslips using a previously described procedure.[7,13] To study the GFAP-dependence of the effects that these two CNT modalities have on the morphological and proliferative properties of astrocytes, we used: (i) SWCNT-PEG dispersion (5 μg/mL) applied to the cells grown on glass coverslips coated with polyethylenimine (PEI), a standard stratum commonly used to promote cell adhesion and growth, and (ii) glass coverslips coated with SWCNT-PEG strata with a film thickness of 60 nm (for detailed characterization of these materials, see refs 4 and 7).

We used purified astrocytes isolated from the visual cortices of GFAP KO mice (for detailed information on the GFAP KO mice see ref 11) and the corresponding background strain, C57BL/6 (wild-type). To confirm the identity of purified cells

dx.doi.org/10.1021/nl4048114 | Nano Lett. 2014, 14, 3720–3727

as astrocytes, they were plated onto the PEI-coated coverslips and after 3 days in culture incubated with the dipeptide, β-Ala-Lys, conjugated to 7-amino-4-methylcoumarin-3-acetic acid (AMCA) (Supporting Information, Figure S1). This fluorescent probe is specifically taken up by astrocytes and distributes throughout their cytoplasm.[14,15] All the cells isolated from wild-type (n = 23) and GFAP KO (n = 22) mice and studied live accumulated β-Ala-Lys-N_ε-AMCA and hence are astrocytes. To verify GFAP expression, and lack of thereof, wild-type and GFAP KO astrocytes plated onto the PEI-coated coverslips were labeled for GFAP, after 3 days in culture, using indirect immunocytochemistry[4,14] (Figure 1a, left). We also assessed the effects that these CNT modalities have on GFAP-ir of both wild-type and GFAP KO astrocytes (Figure 1a, middle and right). To obtain the total area of the cells (green outline in Figure 1a, bottom), astrocytes were preloaded with β-Ala-Lys-N_ε-AMCA and then fixed. β-Ala-Lys-N_ε-AMCA (data not shown; see e.g., Figure 4 of ref 14) and GFAP-ir of stained wild-type (n = 60) and GFAP KO (n = 47) astrocytes were visualized using a fluorescence microscope, and standard 4′,6-diamidino-2-phenylindole (DAPI) and tetramethylrhodamine isothiocyanate (TRITC) filter sets, respectively. After background subtraction, we quantitatively assessed the GFAP-ir parameters; that is, density (average fluorescence intensity per pixel of the total cell area), content (density × total cell area), and occupancy (positive pixels/total cell area).[4] As expected, we observed that the GFAP KO astrocytes showed a median value close to zero for all the GFAP-ir parameters assessed, implying that the GFAP KO astrocytes do not indeed express GFAP. Furthermore, treating the GFAP KO astrocytes with the SWCNT-PEG solute or plating them onto SWCNT-PEG films did not cause any change in the GFAP-ir parameters (Figure 1b). Wild-type astrocytes, on the other hand, showed significant expression of GFAP. We also observed that the GFAP-ir parameters change when astrocytes interact with the two modalities of CNTs. Astrocytes treated with the SWCNT-PEG solute (5 μg/mL) showed a significant increase in the density along with an increase in the occupancy of GFAP-ir compared to the untreated astrocytes grown on PEI, while an increase in the content of GFAP-ir showed a trend, but did not reach statistical significance (Figure 1b). Astrocytes plated onto the 60 nm thick SWCNT-PEG films showed a significant decrease in the density and content of GFAP-ir, while no significant difference was observed in the occupancy (Figure 1b). Thus, the two modes of CNT presentation produced different changes in the GFAP-ir parameters of wild-type astrocytes (Table 1). Of note, GFAP-ir changes could be due to changes in the protein levels, modification, or conformation and polymerization state of GFAP.[16,17] We used the same concentration of the solute (5 μg/mL) and the same thickness of the films (60 nm) in the entire study, and for clarity we omit textual referral to the concentration/thickness here on.

Changes in the level of GFAP have been linked to changes in the morphology of astrocytes with functional consequences on their physiology.[10] To assess the cellular morphology of wild-type and GFAP KO astrocytes, we plated astrocytes as described in Figure 1, but instead of staining for GFAP we loaded the astrocytes with the vital fluorescent dye, calcein[4,14,18] and imaged them live using a fluorescence microscope with a standard fluorescein isothiocyanate (FITC) filter set (Figure 2a). All the cells plated in the three conditions (n = 160) accumulated calcein, indicating the viability of both wild-type and GFAP KO astrocytes and the biocompatibility of these

Table 1. Summary of the Effects Induced by the Two Modalities of SWCNT-PEG on Cultured Wild-Type (WT) and GFAP Knockout (KO) Astrocytes Compared to those on PEI-Coated Coverslips[a]

		PEI + 5 μg/mL SWCNT-PEG		60 nm SWCNT-PEG Film	
cell property	parameter	WT	KO	WT	KO
GFAP-ir	density	↑	NA	↓	NA
	content	–	NA	↓	NA
	occupancy	↑	NA	–	NA
morphology	area	↑	↑	↑	↑
	perimeter	↑[p]	↑	–	–
	form factor	↓*	–	–	–
vitality	adhesion	–	–	↑	↑
	proliferation	–	–	↑*	–
	death	–*	↑	↓	–

[a]Dash indicates no change, while arrows indicate an increase (up) or decrease (down) in the measurements; NA, not applicable. Asterisk indicates a GFAP-dependent effect; p, partially mediated by GFAP.

CNT modalities. We analyzed the calcein images using a self-designed algorithm[4] to quantitatively assess the morphological parameters of astrocytes by measuring their total cell area and perimeter, which were then used to calculate the form factor (FF),[19] defined by the equation $FF = 4\pi[\text{area}(\mu m^2)]/[\text{perimeter}(\mu m)]^2$. The form factor is a measure of the circularity or the roundness of an object; a perfectly circular/round object has a FF = 1, and a FF ≈ 0 describes a line. We found that both SWCNT-PEG solute and films cause an increase in the area of wild-type and GFAP KO astrocytes compared to the corresponding untreated wild-type and GFAP KO astrocytes plated onto the PEI-coated coverslips (Figure 2b), which implies that GFAP is not necessary for this effect on astrocytes by the CNTs. The perimeter of the wild-type and GFAP KO astrocytes plated onto PEI also showed a significant increase in the presence of the SWCNT-PEG solute, but no significant difference in perimeter was observed when astrocytes were plated onto the SWCNT-PEG films, compared to the corresponding untreated astrocytes plated onto PEI. The SWCNT-PEG solute effect on perimeter was mediated, at least in part, by GFAP as it was significantly less pronounced in GFAP KO astrocytes (Figure 2b). The FF of wild-type astrocytes plated onto PEI showed a significant decrease, i.e., "stellation" of cells, in the presence of the SWCNT-PEG solute, while plating these cells onto the SWCNT-PEG films showed no significant difference compared to that on PEI alone. The SWCNT-PEG solute-induced change in cell shape appears to be a GFAP-dependent process, as the lack of GFAP in the GFAP KO astrocytes occluded this effect (Figure 2b). Of note, astrocytes grown on PEI and treated with PEG solute, at a concentration (1 μg/mL) corresponding to the PEG weight load in SWCNT-PEG, showed no significant changes in the GFAP-ir or morphological parameters when compared to wild-type astrocytes grown on PEI (Supporting Information, Figure S2a–d). These cells showed a trend towards decreased density and content of GFAP-ir when treated with PEG, but this is in the opposite direction of the effect seen for SWCNT-PEG solute. Taken together, these results confirm our previous findings[4,7] that CNTs, applied as colloidal solute or strata, can induce morphological changes in wild-type astrocytes (Table 1). A minor difference is that previously we found a marginally

dx.doi.org/10.1021/nl4048114 | Nano Lett. 2014, 14, 3720–3727

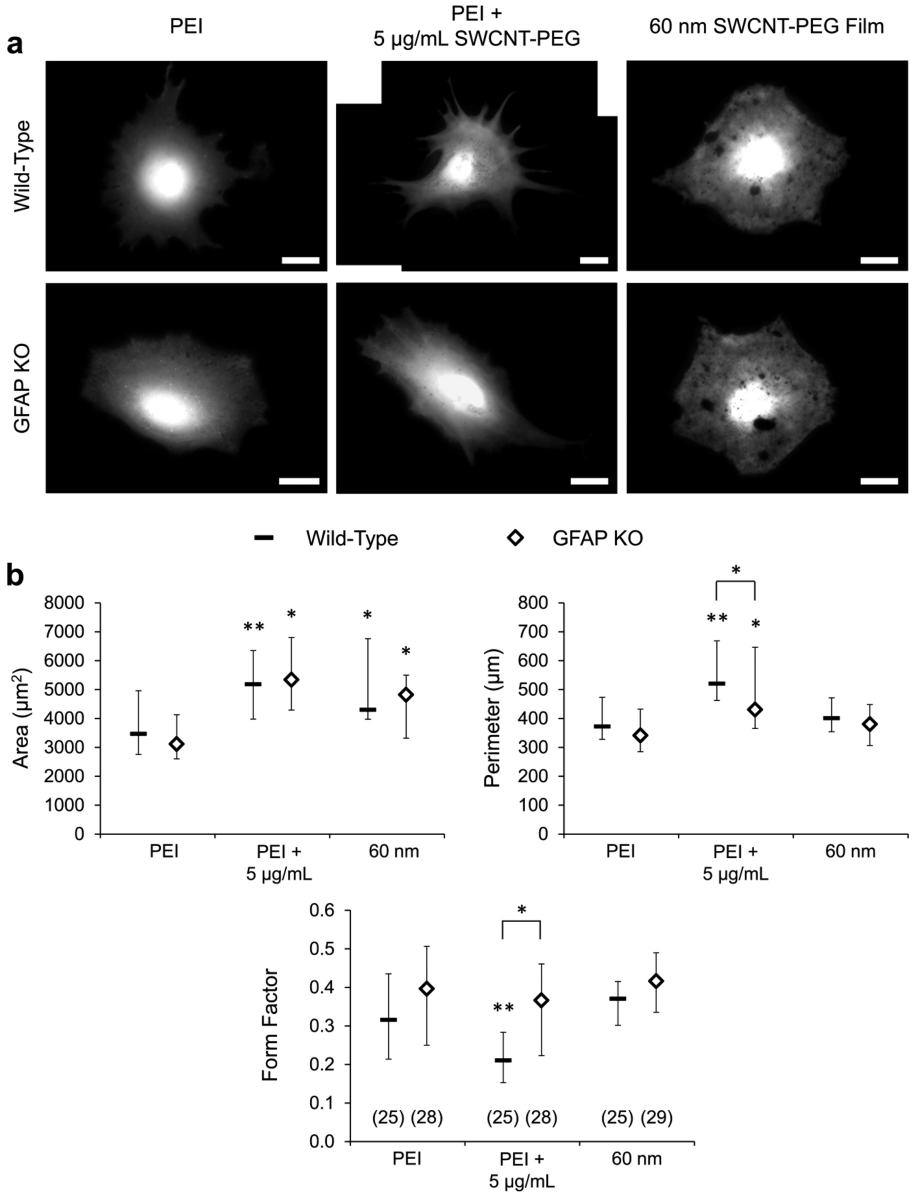

Figure 2. GFAP is necessary for the modulation of a subset of morphological characteristics in astrocytes induced by the CNT modalities. (a) Images of live wild-type and GFAP KO astrocytes in culture plated onto the PEI-coated coverslips in the absence and presence of the SWCNT-PEG solute (5 μg/mL) and onto the 60 nm thick SWCNT-PEG films, loaded with the vital fluorescent dye, calcein. Scale bar, 20 μm. (b) Summary graphs showing the median effects of the CNT modalities on the morphology of astrocytes. The number of astrocytes studied in each condition is given in parentheses in the form factor graph. *p < 0.05, **p < 0.01. Other annotations as in Figure 1.

significant increase in the form factor of the astrocytes plated onto the SWCNT-PEG films compared to that on PEI,[7] whereas in the current set of experiments, the increase did not reach statistical significance. This discrepancy, likely a result of biological variability,[20] does not detract from the main finding here; i.e., that the changes in the perimeter and shape/FF of astrocytes induced by the SWCNT-PEG solute are dependent on GFAP (Table 1).

Changes in the expression/amount of GFAP are often associated with changes in the proliferation of astrocytes.[10] To initially assess the role of GFAP in the proliferation of astrocytes in our cell culture conditions, we plated wild-type and GFAP KO astrocytes onto the PEI-coated coverslips. At 4 h and 4 days postplating, the astrocytes were loaded with calcein, their nuclei labeled with the cell permeable nuclear stain Hoechst 33342 and imaged live using a fluorescence microscope and FITC and DAPI filter sets, respectively (Figure 3a). The 4 h time point gives an estimate on the initial plating density and adhesion of astrocytes, while the 4 day time point gives an estimate on the proliferation of astrocytes.[7] We observed that the wild-type and GFAP KO astrocytes plated onto PEI showed similar median initial plating densities at the 4 h time point of about 23 300 cells per cm^2 and 21 500 cells per cm^2, respectively, which significantly increased to about 36 800 cells per cm^2 and 33 500 cells per cm^2 at the 4 day time point, implying that both groups of astrocytes undergo proliferation in culture (Figure 3b). We also observed that the percentage increase in the number of cells was similar for both wild-type (~58%) and GFAP KO (~56%) astrocytes, implying that the rate of proliferation of astrocytes is not dependent on GFAP when plated on our reference stratum.

dx.doi.org/10.1021/nl4048114 | Nano Lett. 2014, 14, 3720−3727

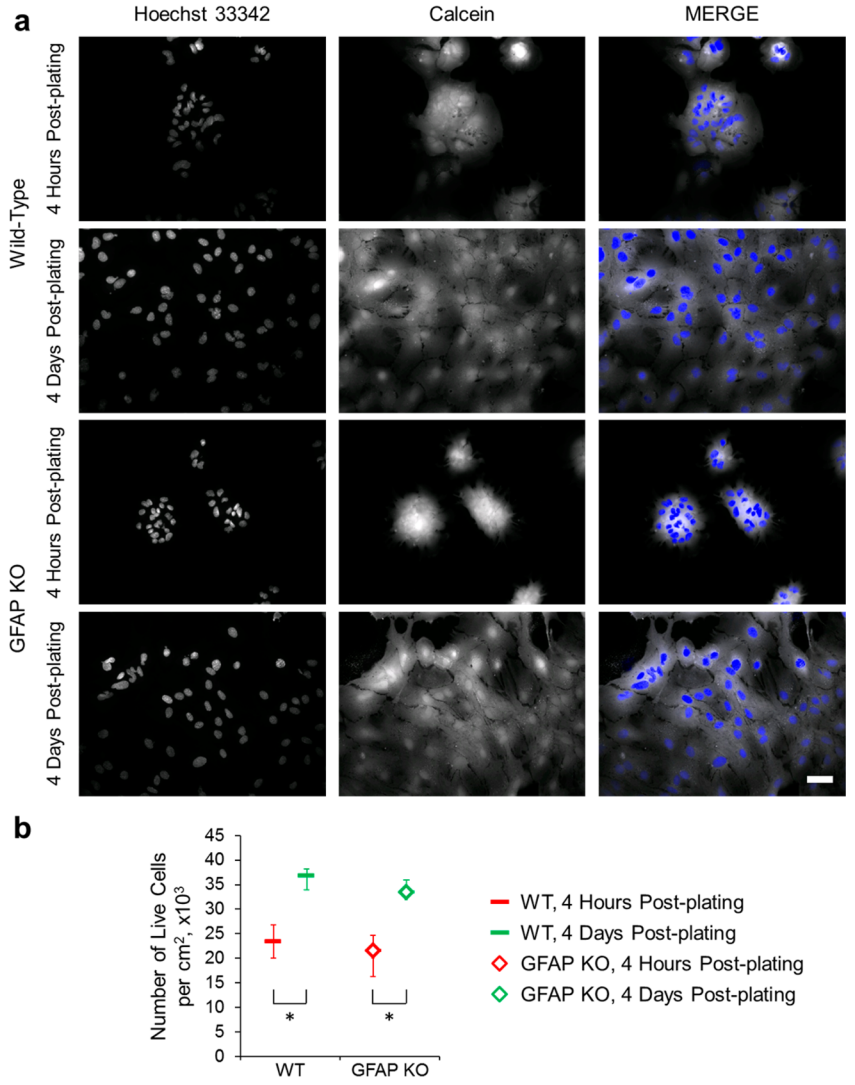

Figure 3. Untreated wild-type and GFAP KO astrocytes show similar adhesive and proliferative characteristics in culture. (a) Images of astrocytic nuclei labeled with the cell permeable nuclear dye, Hoechst 33342, (left column) and the corresponding astrocytes loaded with the vital fluorescent dye, calcein (middle column). Right column shows the merge of the images. Top two and bottom two rows show the images of wild-type and GFAP KO astrocytes, respectively, plated onto the PEI-coated coverslips, 4 h and 4 days postplating. Scale bar, 50 μm. (b) Summary graph showing the median number (with IQR) of live cells per cm^2 on the PEI-coated coverslips, 4 h (marked in red) and 4 days (marked in green) postplating. The Mann−Whitney U-test was used for the comparison between wild-type and GFAP KO astrocytes at each time point. The Wilcoxon signed-rank test was used for the comparison between the time points in each group (wild-type or GFAP KO astrocytes); the differences are marked by the brackets. *$p < 0.05$.

Having determined the proliferation parameters of astrocytes grown on PEI, we treated wild-type astrocytes grown on PEI-coated coverslips with the SWCNT-PEG solute or PEG (Supporting Information, Figure S2e) and also plated them onto the SWCNT-PEG films (Supporting Information, Figure S3). Similarly, we also exposed GFAP KO astrocytes to these two different modalities of CNTs (Supporting Information, Figure S4). We then calculated the relative density of live cells across the different groups (astrocyte type) and conditions (CNT modalities) by normalizing the number of live cells in each group, condition, and time point to the median number of live wild-type astrocytes on the PEI-coated coverslips at 4 h postplating (Figure 4a). We found that the relative densities of live wild-type astrocytes present on the PEI-coated coverslips were similar in the absence and presence of the SWCNT-PEG solute at both the 4 h and 4 day time points, albeit there were significantly more astrocytes at the 4 day time point compared to the 4 h time point due to cell proliferation (Figure 4a, Table 1). Similar results were obtained when wild-type astrocytes grown on the PEI-coated coverslips were treated with PEG (Supporting Figure S2e). However, when astrocytes were grown on the SWCNT-PEG films, they had higher densities at the 4 h time point than the astrocytes grown on PEI, presumably due to enhanced cellular adhesion onto the CNT films. Furthermore, proliferation (fold-increase) of wild-type astrocytes on the CNT films was higher than that for astrocytes grown on PEI alone (Figure 4a, Table 1). These effects of SWCNT-PEG films on astrocyte adhesion and proliferation are in agreement with our previous work.[7] GFAP KO astrocytes grown on PEI and treated with the SWCNT-PEG solute showed similar adhesive and proliferative characteristics as wild-type astrocytes (Figure 4a). They also showed enhanced adhesion when plated on the SWCNT-PEG films; but unlike the wild-type astrocytes, the films did not enhance their

dx.doi.org/10.1021/nl4048114 | Nano Lett. 2014, 14, 3720−3727

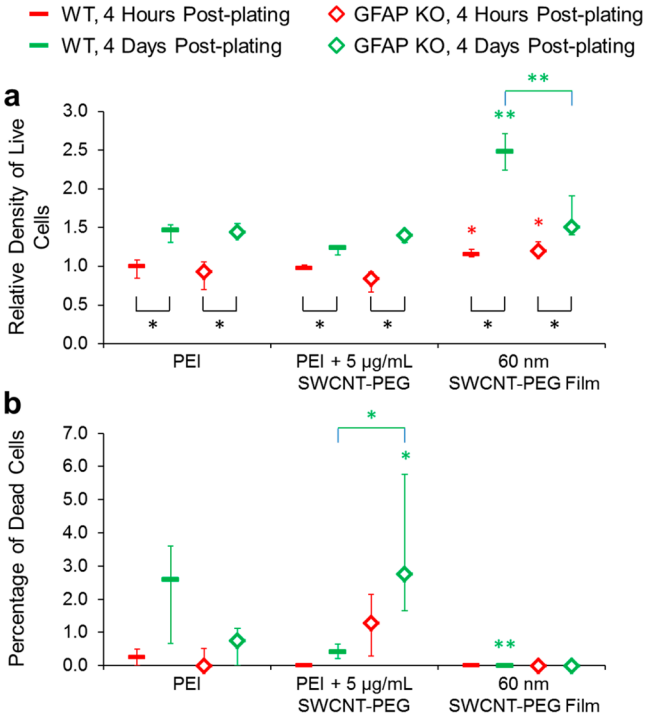

Figure 4. GFAP is necessary for the modulation of a subset of proliferative characteristics and astrocyte death induced by the CNT modalities. (a) Summary graph showing the median relative density of live cells present on the PEI-coated coverslips in the absence and presence of the SWCNT-PEG solute (5 μg/mL) and onto the 60 nm thick SWCNT-PEG films, normalized to the median number of live wild-type astrocytes at 4 h postplating on the PEI-coated coverslips. (b) Summary graph showing the median percentage of dead cells in the above setting. We used seven coverslips per data point. The KWA followed by the Newman–Keuls' test was used for the comparison between the different conditions (CNT modalities) in each group (wild-type or GFAP KO astrocytes) and time point; asterisks indicate a statistical difference when compared to the cells plated onto the PEI-coated coverslips within the same group and time point. The Wilcoxon signed-rank test was used for the comparison between the time points in each group, and the Mann–Whitney U-test was used for the comparison between the groups in each condition and time point; differences are marked with brackets. *$p < 0.05$, **$p < 0.01$. Other annotations as in Figure 3.

proliferation compared to the astrocytes grown on PEI (Figure 4a). This finding implies specifically that the enhancement of proliferation, but not adhesion, induced by the SWCNT-PEG films is dependent on GFAP (Table 1).

The percentage of dead wild-type astrocytes across the conditions showed no significant differences at the 4 h time point, but it was significantly lower at the 4 day time point for the cells plated onto the SWCNT-PEG films compared to that on PEI (Figure 4b). This latter finding is an extension of the previously observed trend.[7] GFAP KO astrocytes also showed no significant differences in the percentage of dead cells across conditions at the 4 h time point, while the percentage was significantly higher at the 4 day time point for the cells plated onto PEI in the presence of the SWCNT-PEG solute than in its absence. This percentage of dead GFAP KO cells plated onto PEI and treated with the SWCNT-PEG solute was also significantly higher compared to the corresponding condition in wild-type astrocytes. This finding may indicate that the presence of GFAP in wild-type astrocytes protects them from a previously unappreciated harmful effect of the SWCNT-PEG solute (Table 1). Of note, there was a significantly higher proportion of dead wild-type astrocytes grown on PEI in the presence of PEG at 4 d vs 4 h postplating, albeit the death toll at either time point was not different from that of control astrocytes grown on PEI in the absence of PEG (Supporting Figure S2e).

In this study, we show that GFAP has a dual role in the morpho-proliferative changes of astrocytes induced by the two modalities of CNTs using a GFAP KO mouse model (Table 1). Although it is plausible that the deletion of GFAP could potentially lead to changes in the expression of other astrocytic proteins, it is the absence of GFAP that directly and/or indirectly modulates the cellular changes induced by the two modalities of CNTs. The changes in GFAP-ir in wild-type astrocytes, that occur upon exposure to the solute or film forms of SWCNT-PEG, appear causally unrelated to the increase in cell area (Figure 2b), as a similar effect on area is also seen in GFAP KO astrocytes. In contrast, GFAP does contribute to the other CNT-induced morphological effects on astrocytes. Hence, an increase in the density/occupancy of GFAP-ir in wild-type astrocytes treated with the SWCNT-PEG solute seems critical for an increase in cell perimeter and a change in cell shape (a decrease in form factor), as these CNT-induced effects are mitigated or obliterated, respectively, in GFAP KO astrocytes (Figure 2b). It should be noted, however, that a decrease in GFAP density/content in wild-type astrocytes and a complete absence of this protein in GFAP KO astrocytes when grown on CNT films (Figure 1b) neither affects cell perimeter nor cell shape (Figure 2b). This dichotomy in the effects of GFAP indicates that soluble SWCNTs induce morphological changes in astrocytes by a different signaling pathway than SWCNT films, with GFAP participating in the former but not the latter.

The effects induced by the SWCNT-PEG colloidal solute are not due to the PEG functional group, but rather due to the CNT itself (Supporting Information, Figure S2). This is in agreement with our previous findings showing that SWCNTs covalently linked to two different functional groups, PEG or poly-*m*-aminobenzenesulfonic acid, both of which render them water-soluble, induce qualitatively similar effects on the properties of neurons and astrocytes in culture, implying that the CNT backbone is responsible for the changes in the cellular properties induced by the water-soluble SWCNTs.[3,4]

The dichotomy in the effects of GFAP is further supported by the effects of SWCNTs on the adhesion and proliferative characteristics of astrocytes (Table 1). There was no effect of the absence of GFAP on the increased adhesion of astrocytes to SWCNT-PEG films compared to PEI alone (Figure 4a, 4 h time point); however, the presence of GFAP was required for the enhanced proliferation on SWCNT-PEG films when compared to PEI alone (Figure 4a, 4 day time point).

Astrocytes exposed to SWCNT-PEG solute show some similarities to reactive astrocytes, including increased size (area and perimeter), stellation (decreased form factor), and GFAP-ir, as we previously observed.[4] The reactive state of astrocytes is considered a fundamental adaptive/defensive reaction of the neural tissue to an insult; for example, reactive astrocytes have been shown to provide protection and preservation of spinal cord tissue and its functions after a moderate spinal cord injury.[21] GFAP null astrocytes plated onto PEI in the presence of soluble SWCNT-PEG have a higher percentage of dead cells than wild-type astrocytes, suggesting the presence of a previously unrecognized toxic effect of soluble SWCNTs for

dx.doi.org/10.1021/nl4048114 | *Nano Lett.* 2014, 14, 3720–3727

which GFAP offers protection (Figure 4b). This toxic effect is quite modest, however, affecting only a small fraction (~3%) of the GFAP KO astrocytes, and having no significant effect on the relative density of live astrocytes (Figure 4a). Thus, a previously proposed potential use of SWCNT-PEG solutes in the treatment/prevention of neurodegenerative diseases with astrocytic atrophy,[4] such as a hereditary form of Alzheimer's disease characterized by a decrease in the volume of GFAP profiles and reduction of astrocytic arborization,[22] remains a valid lead for translational biomedicine.

Astrocytes grown on SWCNT-PEG films, with their decrease in GFAP-ir and increased proliferation, have similarities to dedifferentiated neural stem cells; i.e., type B cells, which are precursors giving rise to neuroblasts,[23] as we previously observed.[7] It is plausible that this effect could also be seen on the astrocytes present at the interface of BMI electrodes coated with CNTs.

Although different CNT modalities have shown great promise in neural prosthesis,[5,9,24] care should be taken when using them in different biomedical applications, as in some conditions they can lead to neurotoxicity.[25,26] Therefore, it is important to assess the effects that different CNT modalities may have on the brain, including signaling within and between neural cells, to establish exposure limits and safety guidelines for the use of this promising nanomaterial in neural applications in the near future.

Methods Summary. We described methods in details elsewhere;[4,7] here we only provide an essential summary of the methods used in the present study and specifically point out some modifications. Astrocytes isolated from the visual cortices of 0−2-day-old C57BL/6 (wild-type) or GFAP KO mice were purified and maintained in cell culture as we previously described.[4,7] Experimental protocols were approved by the Institutional Animal Care and Use Committee at the University of Alabama at Birmingham.

SWCNT-PEG solutes and 60 nm thick SWCNT-PEG films were synthesized and characterized as we previously described.[4,7] SWCNT-PEG in this study contained 16.0−16.1 wt % PEG. In experiments using PEG solute, as a control for 5 μg/mL of SWCNT-PEG solute treated group, PEG was added to the cells at 1 μg/mL, i.e., at the concentration corresponding to 20 wt % of SWCNT-PEG.

All imaging experiments were done at room temperature (22−25 °C) using a light microscope (Nikon TE300) equipped with differential interference contrast (DIC) and epifluorescence illumination (halogen and xenon arc lamps, respectively; 100 W). To acquire the images, we used either a CoolSNAP-HQ or a CoolSNAP-HQ^2 (for Supporting Information Figure S2 only) cooled, charge coupled device camera (Photometrics, Tucson, AZ) driven by MetaMorph imaging software ver. 6.1 (Molecular Devices, Chicago, IL). All the raw fluorescence images had pixel intensities without saturation and within the dynamic range of the camera (0−4095 for CoolSNAP-HQ or 0−16383 for CoolSNAP-HQ^2). Astrocytes were loaded with β-Ala-Lys-N_ε-AMCA (20 μM at 37 °C for 1 h in cell culture medium), and the coverslips containing the cells were rinsed in the external solution, mounted onto an imaging chamber filled with external solution, and examined live using a standard DAPI filter set and a 60× Plan Apo objective (numerical aperture, 1.4) as described elsewhere.[14,15] External solution contained (in mM): NaCl (140), KCl (5), $CaCl_2$ (2), $MgCl_2$ (2), D-glucose (5), and Hepes (10) (pH 7.4). Alternatively, β-Ala-Lys-N_ε-AMCA loaded astrocytes were subjected to indirect immunocytochemistry. They were subsequently fixed and labeled for GFAP (mouse monoclonal, 1:500 dilution; ICN Cat. No. 69110; MP Biomedicals; Solon, OH; followed by a TRITC-conjugated secondary antibody)[7] and analyzed for the cell area by manual tracing (based on the β-Ala-Lys-N_ε-AMCA images acquired using a standard DAPI filter set), and for the density, content, and occupancy of GFAP-ir based on the images acquired using a standard TRITC filter set and a 60× Plan Apo objective (numerical aperture, 1.4).[4] To test for the nonspecific binding of the secondary antibody and cellular autofluorescence, parallel controls were run, in which the primary antibody was omitted. GFAP positive pixels were identified as described elsewhere.[4] Briefly, all the images of astrocytes (exposed and not exposed to the primary antibody) were background subtracted; background fluorescence was obtained from regions of coverslips containing no cells. Mean intensity plus six standard deviations of the background subtracted images of astrocytes not exposed to the primary antibody was used to calculate a threshold value for GFAP positive pixels. As in the previous work, only the astrocytes that could be imaged within a single frame were analyzed in order to avoid errors in the quantification of fluorescence intensity that would otherwise occur during the stitching/autoleveling step in morphometric analysis (see below). The only difference in the current study is that the coverslips (thickness no. 1) with the astrocytes were mounted onto coverglasses (thickness no. 1) instead of glass microscopic slides and imaged through the coverglasses, to avoid assessment of any possible errors associated with the absorption of light by the CNT films themselves (see Figures S6, S9 of ref 7).

To quantify astrocytic morphological changes, cells were loaded with calcein (1 μg/mL calcein-AM with 0.025% w/v pluronic acid, Invitrogen; 15 min) and, after de-esterification (15 min), imaged live bathed in external solution; a standard FITC filter set and a 60× Plan Apo objective (numerical aperture, 1.4) were used for the visualization of calcein fluorescence, as we described elsewhere in detail.[4,14,18] The area and perimeter of the cells were obtained using a self-designed algorithm, involving the stitching/autoleveling step when needed (see Figure S1 of ref 4), which were further used to calculate the FF as we described elsewhere.[4]

In experiments assessing the adhesive and proliferative characteristics of astrocytes, nuclei of calcein-loaded astrocytes were labeled with Hoechst 33342 trihydrochloride trihydrate (5 μg/mL, 15 min; Invitrogen). Imaging of live astrocytes was done using standard FITC (calcein) and DAPI (Hoechst) filter sets and a 20× Plan Fluor objective, 4 h and 4 days postplating. The number of nuclei per view field (0.15 mm^2) were counted as we described in detail elsewhere.[7] The cells positive for Hoechst and calcein were considered live, while the cells positive for Hoechst and negative for calcein were considered dead.

Statistical analysis was done using the GB-Stat v6.5 software (Dynamic Microsystems Inc., Silver Spring, MD) and SAS Software, version 9.2 of the SAS software for Windows (SAS Institute Inc., Cary, NC). The number of subjects required for individual set of experiments was estimated using power analysis (set at 80% and $\alpha = 0.05$). Since some of the subgroups deviated from normality based on the Shapiro−Wilk test for normality, we used nonparametric statistics. In all the experiments, the Mann−Whitney U-test was used for the comparison between wild-type and GFAP KO astrocytes in

dx.doi.org/10.1021/nl4048114 | Nano Lett. 2014, 14, 3720−3727

each condition. To test the difference between the 4 h and 4 day time points in the proliferation study, the two correlated groups were compared using the Wilcoxon signed-rank test (Figures 3 and 4). For all the other experiments with comparison between the different conditions in the same group, the multiple independent conditions were analyzed using the Kruskal–Wallis one-way ANOVA (KWA) followed by the Dunn's or the Newman–Keuls' test to assess a statistical significance (established at $p < 0.05$) in the effect induced by the CNT modalities when compared to PEI. The Mann–Whitney U-test was used for the comparison of morpho-functional properties between the untreated and PEG treated wild-type astrocytes (Supporting Information, Figure S2a–d); the sole exception was the use of the Student's t test for the assessment of the form factor.

■ ASSOCIATED CONTENT

Supporting Information

Figures S1–S4. This material is available free of charge via the Internet at http://pubs.acs.org.

■ AUTHOR INFORMATION

Corresponding Authors

*E-mail: vlad@uab.edu.

*E-mail: robert.haddon@ucr.edu.

Author Contributions

V.P., R.C.H., and M.B. were responsible for the overall project conception, design, and supervision. M.K.G. and V.P. designed the experiments. E.B. characterized the CNTs. M.B. provided the GFAP KO mice used in the study. M.K.G. performed all the experiments on astrocytes and analyzed the data. M.K.G. and V.P. wrote the paper. All authors discussed the results and commented on the manuscript.

Notes

The authors declare no competing financial interest.

■ ACKNOWLEDGMENTS

We thank Mary Seelig for her assistance in maintaining the mice colony. V.P. acknowledges the support of this work by National Institutes of Health (The Eunice Kennedy Shriver National Institute of Child Health and Human Development award HD078678).

■ REFERENCES

(1) Bekyarova, E.; Ni, Y.; Malarkey, E. B.; Montana, V.; McWilliams, J. L.; Haddon, R. C.; Parpura, V. *J. Biomed. Nanotechnol.* **2005**, *1* (1), 3–17.

(2) Malarkey, E. B.; Parpura, V. *Neurodegener. Dis.* **2007**, *4* (4), 292–9.

(3) Ni, Y.; Hu, H.; Malarkey, E. B.; Zhao, B.; Montana, V.; Haddon, R. C.; Parpura, V. *J. Nanosci. Nanotechnol.* **2005**, *5* (10), 1707–12.

(4) Gottipati, M. K.; Kalinina, I.; Bekyarova, E.; Haddon, R. C.; Parpura, V. *Nano Lett.* **2012**, *12* (9), 4742–7.

(5) Roman, J. A.; Niedzielko, T. L.; Haddon, R. C.; Parpura, V.; Floyd, C. L. *J. Neurotrauma* **2011**, *28* (11), 2349–62.

(6) Malarkey, E. B.; Fisher, K. A.; Bekyarova, E.; Liu, W.; Haddon, R. C.; Parpura, V. *Nano Lett.* **2009**, *9* (1), 264–8.

(7) Gottipati, M. K.; Samuelson, J. J.; Kalinina, I.; Bekyarova, E.; Haddon, R. C.; Parpura, V. *Nano Lett.* **2013**, *13* (9), 4387–92.

(8) Ansaldo, A.; Castagnola, E.; Maggiolini, E.; Fadiga, L.; Ricci, D. *ACS Nano* **2011**, *5* (3), 2206–14.

(9) Keefer, E. W.; Botterman, B. R.; Romero, M. I.; Rossi, A. F.; Gross, G. W. *Nat. Nanotechnol.* **2008**, *3* (7), 434–9.

(10) Brenner, M. *Neurosci. Lett.* **2014**, *565*, 7–13.

(11) McCall, M. A.; Gregg, R. G.; Behringer, R. R.; Brenner, M.; Delaney, C. L.; Galbreath, E. J.; Zhang, C. L.; Pearce, R. A.; Chiu, S. Y.; Messing, A. *Proc. Natl. Acad. Sci. U.S.A.* **1996**, *93* (13), 6361–6.

(12) Zhao, B.; Hu, H.; Perea, D.; Haddon, R. C. *J. Am. Chem. Soc.* **2005**, *127*, 8197–8203.

(13) Bekyarova, E.; Itkis, M. E.; Cabrera, N.; Zhao, B.; Yu, A.; Gao, J.; Haddon, R. C. *J. Am. Chem. Soc.* **2005**, *127*, 5990–5995.

(14) Montana, V.; Ni, Y.; Sunjara, V.; Hua, X.; Parpura, V. *J. Neurosci.* **2004**, *24* (11), 2633–42.

(15) Malarkey, E. B.; Ni, Y.; Parpura, V. *Glia* **2008**, *56* (8), 821–35.

(16) Le Prince, G.; Fages, C.; Rolland, B.; Nunez, J.; Tardy, M. *Glia* **1991**, *4* (3), 322–6.

(17) Wang, Y. F.; Hatton, G. I. *J. Neurosci.* **2009**, *29* (6), 1743–54.

(18) Reyes, R. C.; Perry, G.; Lesort, M.; Parpura, V. *Cell Calcium* **2011**, *49* (1), 23–34.

(19) Wilms, H.; Hartmann, D.; Sievers, J. *Cell Tissue Res.* **1997**, *287* (3), 447–58.

(20) Hu, H.; Ni, Y.; Mandal, S. K.; Montana, V.; Zhao, B.; Haddon, R. C.; Parpura, V. *J. Phys. Chem. B* **2005**, *109* (10), 4285–9.

(21) Faulkner, J. R.; Herrmann, J. E.; Woo, M. J.; Tansey, K. E.; Doan, N. B.; Sofroniew, M. V. *J. Neurosci.* **2004**, *24* (9), 2143–55.

(22) Yeh, C. Y.; Vadhwana, B.; Verkhratsky, A.; Rodriguez, J. J. *ASN Neuro* **2011**, *3* (5), 271–9.

(23) Doetsch, F.; Caille, I.; Lim, D. A.; Garcia-Verdugo, J. M.; Alvarez-Buylla, A. *Cell* **1999**, *97* (6), 703–16.

(24) Lee, H. J.; Park, J.; Yoon, O. J.; Kim, H. W.; Lee do, Y.; Kim do, H.; Lee, W. B.; Lee, N. E.; Bonventre, J. V.; Kim, S. S. *Nat. Nanotechnol.* **2011**, *6* (2), 121–5.

(25) Belyanskaya, L.; Weigel, S.; Hirsch, C.; Tobler, U.; Krug, H. F.; Wick, P. *Neurotoxicology* **2009**, *30* (4), 702–11.

(26) Wick, P.; Manser, P.; Limbach, L. K.; Dettlaff-Weglikowska, U.; Krumeich, F.; Roth, S.; Stark, W. J.; Bruinink, A. *Toxicol. Lett.* **2007**, *168* (2), 121–31.